Kinetic Study of the ClOO + NO Reaction Using Cavity Ring-Down Spectroscopy

Shinichi Enami, Yosuke Hoshino, Yuki Ito, Satoshi Hashimoto, and Masahiro Kawasaki*
Department of Molecular Engineering and Graduate School of Global Environmental Studies, Kyoto University, Kyoto 615-8510, Japan

Timothy J. Wallington
Scientific Research Laboratories, Ford Motor Company, Dearborn, Michigan 48121-2053
Received: May 23, 2005; In Final Form: December 12, 2005

Cavity ring-down spectroscopy was used to study the reaction of ClOO with NO in 50−150 Torr total pressure of O_2/N_2 diluent at 205−243 K. A value of $k(ClOO+NO) = (4.5 \pm 0.9) \times 10^{-11}$ cm^3 molecule^{-1} s^{-1} at 213 K was determined (quoted uncertainties are two standard deviations). The yield of NO_2 in the ClOO + NO reaction was 0.18 ± 0.02 at 213 K and 0.15 ± 0.02 at 223 K. An upper limit of $k(ClOO+Cl_2) < 3.5 \times 10^{-14}$ cm^3 molecule^{-1} s^{-1} was established at 213 K. Results are discussed with respect to the atmospheric chemistry of ClOO and other peroxy radicals.

1. Introduction

ClOO is a weakly bound species (Cl−O bond strength, 19.5 kJ mol^{-1}), which exists in rapid equilibrium with Cl atoms and O_2, $K_p(T) = k_1/k_{-1} = (1.04 \pm 0.04) \times 10^{-5} \exp((2668 \pm 25)/T)$ bar^{-1}.[1−7]

$$Cl + O_2 + M \rightleftarrows ClOO + M \qquad (1, -1)$$

In the troposphere, the [ClOO]/[Cl] ratio increases from approximately 2% near the Earth's surface to 8% at 12 km, reflecting the dominant effect of decreased temperature (as opposed to decreased $[O_2]$) with increased altitude on the equilibrium. For altitudes above 12 km the effects of increasing temperature and decreasing $[O_2]$ reinforce each other resulting in a steadily decreasing [ClOO]/[Cl] ratio with increasing altitude ([ClOO]/[Cl] ≈ 1% at 25 km, ≈ 0.1% at 35 km).[8,9]

Peroxy radicals of the general formula RO_2 (e.g., HO_2, CH_3O_2, $C_2H_5O_2$, etc.) are key intermediates in the atmospheric chemistry of all organic compounds. The reaction of RO_2 with NO is particularly important in the chemistry responsible for the formation of urban air pollution. ClOO provides an interesting example of a peroxy radical that is weakly bound and unstable at room temperature. Information concerning the kinetics and mechanisms of reactions of ClOO radicals provides useful insight into the atmospheric chemistry of peroxy radicals in general. Although the kinetics of the ClOO self-reaction and its reaction with Cl atoms are reasonably well understood,[10−12] there have been few studies of the kinetics and mechanisms of reactions of ClOO radicals with other atmospherically relevant species. For example, the ClOO + NO reaction has three thermochemically allowed reaction channels, but the kinetics and mechanism of this reaction have yet to be studied.

$$ClOO + NO \rightarrow ClO + NO_2 \qquad \Delta H = -53 \text{ kJ mol}^{-1} \qquad (2a)$$

$$ClOO + NO \rightarrow ClNO + O_2 \qquad \Delta H = -136 \text{ kJ mol}^{-1} \qquad (2b)$$

$$ClOO + NO + M \rightarrow ClONO_2 + M \qquad \Delta H = -165 \text{ kJ mol}^{-1} \qquad (2c)$$

We have used cavity ring-down spectroscopic techniques to study (i) the kinetics of the ClOO + NO and ClOO + Cl_2 reactions in 50−150 Torr of O_2/N_2 diluent at 205−243 K, and (ii) the NO_2 yield from the ClOO + NO reaction at 213−243 K. The present work had two goals. First, to provide kinetic and mechanistic for the reaction of ClOO with NO that can be used to shed light on the chemistry of other peroxy radicals. Second, to extend the utility of the time-resolved cavity ring-down technique by demonstrating its application to study ClOO radical kinetics.

2. Experimental Section

2.1. Kinetic Study of ClOO + Cl_2 and ClOO + NO Reactions. Cavity ring-down spectroscopy (CRDS) was first introduced by O'Keefe and Deacon[13] and has been applied widely in spectroscopic and kinetic studies.[14,15] The technique is based on monitoring the decay of a laser pulse trapped in an optical cavity. The presence of absorbing species within the cavity increases the decay rate (shortens the ring-down time) of the intensity of the laser pulse within the cavity. Measurement of the ring-down time provides information on the strength of absorption within the cavity. Lin and co-workers[16] reported the first application of CRDS to kinetic studies by combining CRDS with laser flash photolysis. Lin and co-workers derived kinetic data for reactions of phenyl radicals by monitoring ring-down time as a function of delay between photolysis and probe laser pulses in a technique called "time-resolved CRDS"[16,17] Over the past decade, time-resolved CRDS has been used by several research groups in kinetic studies of a variety of species, e.g., FCO,[18] CHO,[19] BrO,[20] IO,[21] C_2H_5,[22] $C_2H_5O_2$,[22] and NO_3.[23]

Figure 1a shows a schematic diagram of the time-resolved CRDS apparatus used in the present study. The system employs pulsed photolysis and probe lasers. After the photolysis laser beam traverses a Pyrex glass tube reactor (21 mm i.d.), the probe laser beam is injected nearly collinear to the axis of the photolysis laser through one of two high-reflectivity mirrors (Research Electro-Optics, reflectivity > 0.999 at 266 nm). Light

* To whom corresponding should be addressed. Fax number: + 81-75-383-2573. E-mail address; kawasaki@moleng.kyoto-u.ac.jp.

10.1021/jp052688d CCC: $33.50
Published on Web 02/11/2006

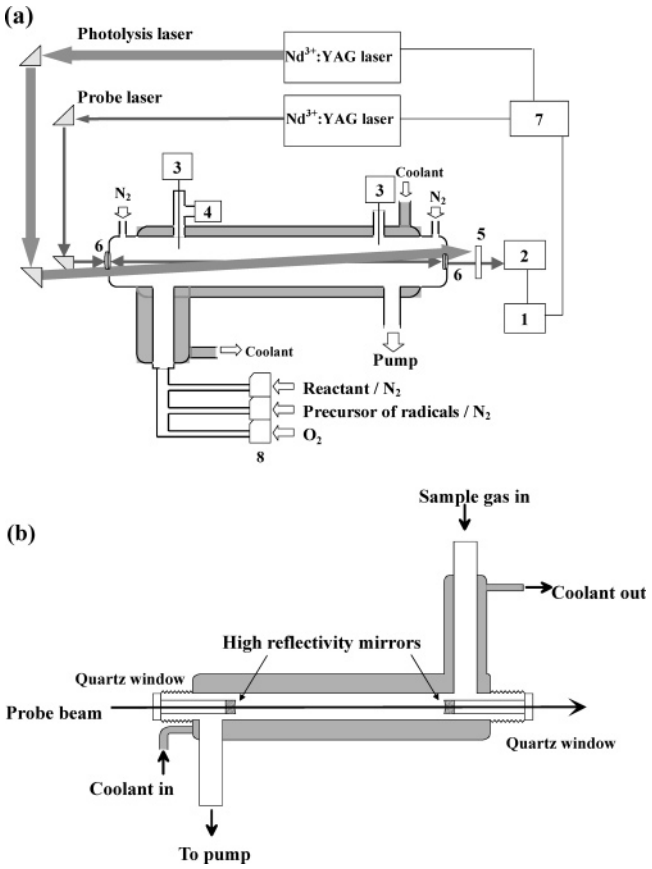

Figure 1. Schematic diagrams of CRDS systems used in the kinetic (a) and spectroscopic (b) studies. Labeled components in (a): 1, digital oscilloscope; 2, photomultiplier; 3, thermometer; 4, pressure gauge; 5, band-pass filter; 6, high-reflective mirrors; 7, delay generator; 8, mass flow controller.

leaking from the exit mirror was detected by a photomultiplier tube (Hamamatsu Photonics, R212UH) through suitable narrow band-pass filters (Edmund Optics) to reduce scattered light from the 355 nm photolysis laser pulse. Decay profiles of the light intensity were recorded using a digital oscilloscope (Tektronix, TDL-714L, 8-bit digitizer) and transferred to a personal computer. In the presence of an absorbing species, the light intensity within the cavity is given by

$$I(t) = I_0 \exp(-t/\tau) = I_0 \exp(-t/\tau_0 - \sigma n c L_R t/L_C) \quad (3)$$

where I_0 and $I(t)$ are the light intensities at time 0 and t, τ is the cavity ring-down time with photolysis beam, τ_0 is the cavity ring-down time without photolysis laser light (typically 1.5 μs), L_R is the length of the reaction region (400 $\pm$ 10 mm), L_C is the cavity length (1040 mm), c is the velocity of light, and n and σ are the concentration and the absorption cross section of absorbing species. A value of $\sigma(\mathrm{ClOO}) = 9.05 \times 10^{-18}$ cm^2 molecule^{-1} at 266 nm[11] was used to calculate the absolute concentration of ClOO. By varying the delay between the photolysis and probe laser pulses, the concentration of ClOO could be monitored as a function of time.

The 355 nm output of a Nd^{3+}:YAG laser (Lambda Physik, LPY400) was used to dissociate Cl_2 to generate Cl atoms which then react with O_2 to give ClOO. The photolysis laser was operated with a typical power of 10 mJ/pulse at a repetition rate of 2 Hz. Shot-to-shot fluctuation of the laser power was less than 10%. Absorption by ClOO at 266 nm was monitored (at various delay times with respect to the photolysis laser pulse) with a Nd^{3+}:YAG laser beam (Spectra-Physics, Lab 130).

The temperature of the gas flow region in the glass tube reactor was controlled over the range 205−298 K. The difference between the sample gas temperatures at the entrance and the exit of the gas flow region was <1 K. Typical conditions for decay measurements were total flow rate 1000−4500 cm^3 min^{-1} (STP), $[Cl_2] = 10^{14}-10^{16}$ molecule cm^{-3}, and $[NO] = 10^{14}-10^{15}$ molecule cm^{-3}. Fluctuations of the total pressure, gas flow rates, and temperature in the reaction cell during an experiment were less than 1%, 3%, and 1%, respectively. ClOO decay profiles were measured 30−1000 μs after the photolysis laser pulse. NO_2 and ClNO are expected products of reaction 2. NO_2 and ClNO have modest absorption cross sections in the region 485−491 nm ($\sigma = 10^{-19}-10^{-20}$ cm^2 molecule^{-1}). To monitor the formation of NO_2 and ClNO from reaction 2, it was desirable to use higher concentrations of Cl_2 (typically $10^{16}-10^{17}$ molecule cm^{-3}) than used in the kinetic experiments to generate larger concentrations of ClOO.

To determine the initial Cl atom concentration, $[Cl]_0$, the production of ClO at 273 K was measured at 266 nm using $Cl_2/O_3/O_2$ mixtures with photolysis of Cl_2 at 355 nm and $[Cl_2] = (1-10) \times 10^{15}$ molecule cm^{-3}. Formation of ClOO is negligible at 273 K and Cl atoms are converted quantitatively into ClO radicals via

$$Cl + O_3 \rightarrow ClO + O_2 \quad (4)$$

O_3 was produced by irradiating an oxygen gas flow (slightly higher than 760 Torr) with a low-pressure Hg lamp (Hamamatsu Photonics, L937-02). The initial Cl atom concentration, $[Cl]_0$, calibrated using $\sigma(\mathrm{ClO}) = 5.35 \times 10^{-18}$ cm^2 molecule^{-1} at 266 nm,[8] was observed to increase linearly with $[Cl_2]$. For the low radical concentration employed in the present work dimerization of ClO is not a complication. For experiments at low temperatures, $[Cl]_0$ was calculated using the calibration at 273 K with an appropriate correction for the temperature dependence of the Cl_2 absorption cross section.[8] The initial chlorine atom concentration in the kinetic experiments was $10^{12}-10^{13}$ molecule cm^{-3}.

2.2. Spectroscopic Study for NO_2 Detection. The CRDS cell shown in Figure 1b was used to record low-temperature absorption spectra of NO_2 between 485 and 491 nm using a dye laser (Lambda Physik, ScanMate, spectral resolution < 0.01 nm). The typical concentration of NO_2 was 3.2×10^{14} molecule cm^{-3} and the corresponding τ_0 was 1.5 μs with mirrors (II-VI Optics). As shown in Figure 1b, the two highly reflective mirrors were set into the jacketed region of the cell to keep the gas temperature uniform between the mirrors at $T = 213-243$ K. The cavity length was 550 mm.

Allowance was made for NO_2 dimerization using the reported equilibrium constant in units of cm^3 molecule^{-1}.[8]

$$NO_2 + NO_2 \rightleftarrows N_2O_4 \qquad K_c(T) = 5.2 \times 10^{-29} \exp(6643/T)$$

All reagents were obtained from commercial sources and used without further purification: Cl_2 (high purity, Sumitomo Seika Co.); NO (1.00% in N_2 diluent, Takachiho Co.); NO_2 (99.9%, Teisan Co.); N_2 (99.999%, Teisan Co.); O_2 (>99.995%, Teisan Co.).

3. Results

3.1. Measurement of k(ClOO+Cl_2). Prior to the study of k(ClOO+NO), a limited series of experiments was performed using mixtures of $(3-20) \times 10^{15}$ molecule cm^{-3} of Cl_2 and 4×10^{18} molecule cm^{-3} of O_2 in 100 Torr total pressure of N_2 diluent at 213 K to check for ClOO loss via reaction with Cl_2.

In the experiments, $[Cl]_0$ was maintained at a constant value (within 5%) by adjusting the photolysis laser fluence. With $[Cl]_0$ essentially constant, the loss of ClOO via self-reaction and reaction with Cl should be unchanged and any change in the decay of ClOO can be ascribed to reaction with Cl_2. No change in the decay of ClOO was observed as a function of the Cl_2 concentration, from which we derive an upper limit of $k(ClOO+Cl_2) < 3.5 \times 10^{-14}$ cm^3 molecule^{-1} s^{-1}. This result can be compared to the value of $k(ClOO+Cl_2) = 3.4 \times 10^{-12}$ cm^3 molecule^{-1} s^{-1} reported by Baer et al.[10] to explain the fast decay of ClOO observed in their experiments at room temperature. Experimental constraints in the work of Baer et al.[10] precluded variation of $[Cl_2]$ to confirm that the observed ClOO decay was indeed attributable to reaction with Cl_2 and Baer et al.[10] viewed their value as a "tentative determination". In the present work, $[Cl_2]_0$ was varied with no impact on the ClOO decay rate and we conclude that ClOO reacts slowly, if at all, with Cl_2 at 213 K. Our observations suggest that reaction with Cl_2 is not the explanation of the fast decay of ClOO observed at room temperature by Baer et al.[10]

3.2. Measurement of *k*(ClOO+NO). Figure 2 shows typical decay profiles of ClOO observed in the presence and absence of NO in 100 Torr total pressure of N_2 diluent with $[O_2] = 4.5 \times 10^{18}$ molecule cm^{-3} at 205 K. In the absence of NO, ClOO radicals are lost via diffusion from the detection region, reaction with Cl, and self-reaction. As seen from the insert in Figure 2, there is a small residual absorption evident at reaction times >0.5 ms which we attribute to absorption by stable products (probably ClNO) formed in the system. For simplicity, in our kinetic analysis, we treated the residual absorption as a background offset and subtracted it from the entire signal trace. In reality, the small absorption by stable products such as ClNO will not be constant but will grow during the decay of ClOO. To quantify the error introduced by our simplified analysis method, the IBM chemical kinetics simulator with the chemical mechanism described below was used to provide simulated absorption traces. Applying our simplified method to treat the small residual absorption led to <1% error in the values of k_2 returned by analyzing the simulated data traces.

The decay of [ClOO] can be analyzed as a sum of first and second-order kinetics.[1,20]

$$ClOO + ClOO \rightarrow \text{products} \quad (5)$$

$$\frac{1}{[ClOO]_t} = \left\{\left(\frac{1}{[ClOO]_0} + \frac{2k_5}{k^{1st}}\right)\exp(k^{1st}t) - \left(\frac{2k_5}{k^{1st}}\right)\right\} \quad (6)$$

where $[ClOO]_0$ is the initial ClOO concentration, $[ClOO]_t$ is the concentration of ClOO at time t, and k^{1st} is the pseudo-first-order rate of loss of ClOO with respect to reaction with NO. Figure 3 shows a plot of k^{1st} versus the NO concentration. As seen from Figure 3, variation of the photolysis laser pulse energy from 7 to 17 mJ pulse^{-1} had no discernible effect on k^{1st}, indicating that the initial ClOO radical concentration does not impact the kinetic analysis. The line through the data in Figure 3 is a linear least-squares analysis and provides information on the kinetics of the reaction of ClOO radicals with NO. In a typical kinetic study, the slope of the regression line in Figure 3 could be equated with the bimolecular rate constant k_2. Unfortunately, in the present work because of the rapid equilibrium between ClOO and Cl and consequent presence of significant concentrations of Cl, it is not possible to simply equate the slope in Figure 3 to k_2.

The presence of Cl atoms gives rise to two complications that must be accounted for before a value of k_2 can be derived.

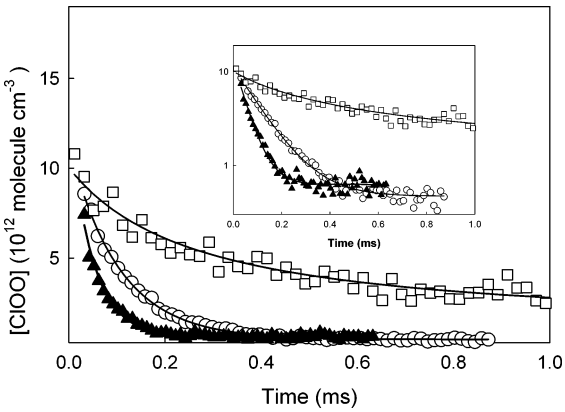

Figure 2. Typical ClOO decay profiles obtained using mixtures containing 3.3×10^{15} of Cl_2 and 4.0×10^{18} molecule cm^{-3} of O_2 in 100 Torr of N_2 diluent at 205 K with [NO] = 0 (squares), 5.1×10^{14} (circles), or 1.4×10^{15} molecule cm^{-3} (filled triangles). The inset shows the same data plotted using a logarithmic *y*-axis scale.

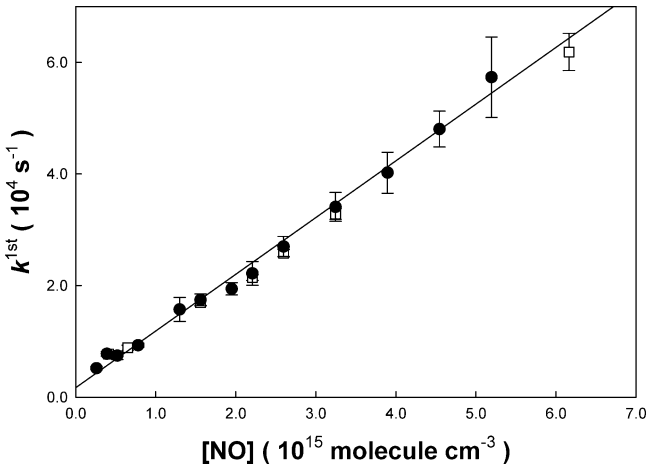

Figure 3. Plot of the pseudo-first-order component of the ClOO decay versus [NO]. Experiments were conducted at 213 K using the following reagent concentrations (molecule cm^{-3}): O_2, 4.0×10^{18}; N_2, 4.7×10^{17}; Cl_2, 3.2×10^{14}; NO, $(2-60) \times 10^{14}$. The photolysis laser fluence was either 7 mJ/pulse (circles) or 17 mJ/pulse (squares).

The first complication is that in addition to ClOO radicals, Cl atoms also react with NO. Loss of Cl atoms via reaction with NO in the system will lead to an enhanced rate of loss of ClOO as the equilibrium (1, −1) shifts to compensate for the lost Cl atoms. To appreciate the magnitude of this effect on the results shown in Figure 3, we must first calculate the fraction of Cl atoms that are present as free Cl atoms compared to those present as ClOO. For the conditions used to obtain the data in Figure 3 ($[O_2] = 4.0 \times 10^{18}$, $[N_2] = 4.7 \times 10^{17}$ molecule cm^{-3}, $T = 213$ K), using $k_1 = 2.7 \times 10^{-33}(T/298)^{-1.5}$ cm^6 molecule^{-2} s^{-1} and $k_{-1} = 2.8 \times 10^{-10}\exp(-1819/T)$ cm^3 molecule^{-1} s^{-1}, it can be calculated that at equilibrium [Cl]/([Cl] + [ClOO]) = 0.75. Using $k(Cl+NO+M) = 9.0 \times 10^{-32}(T/300)^{-1.6}$ cm^6 molecule^{-2} s^{-1},[8] it follows that for $[NO] = 3 \times 10^{15}$ molecule cm^{-3} (a representative [NO] used in our experiments, see Figure 3) the pseudo-first-order loss rate of Cl atoms with respect to reaction with NO is 2100 s^{-1}. This loss rate can be compared to the observed pseudo-first-order loss rate for ClOO in the presence of 3×10^{15} molecule cm^{-3} of NO of approximately 3×10^4 s^{-1}. The loss of Cl atoms via reaction with NO makes a small, but significant, contribution to the observed loss of ClOO.

The second complication is caused by the fact that in all experiments the concentration of Cl atoms exceeds that of ClOO

TABLE 1: Values of k(ClOO+NO) Determined in the Present Work (quoted uncertainties are two standard deviations)

temp (K)	$10^{11}k_{ClOO+NO}$ (cm^3 $molecule^{-1}$ s^{-1})
205	4.3 ± 0.8
213	4.5 ± 0.9
223	4.2 ± 0.8
233	4.9 ± 1.0
243	5.5 ± 1.2

radicals. Loss of ClOO radicals via reaction 2 will be compensated to some degree by reaction of Cl with O_2, generating more ClOO radicals in an attempt to restore the equilibrium. For a system at equilibrium a linear least-squares fit to the measured ClOO loss rates in Figure 3 will underestimate k_2 by a factor of ([ClOO] + [Cl])/[ClOO]. For the conditions relevant to Figure 3 given above ([ClOO] + [Cl])/[ClOO] = 4.1. In reality, the system is not quite at equilibrium and it is necessary to employ a numerical method to compute the necessary correction factors. We constructed a simple chemical mechanism consisting of reactions (1, −1, and 2), simulated the time profile for ClOO using the IBM Chemical Kinetics Simulator Software package, fitted a first-order decay to the profile, and compared the simulated pseudo-first-order decay, k^{first}(sim), to that expected in the absence of problems caused by the (1, −1) equilibrium, k_2[NO]. Correction factors, k_2[NO]/k^{first}(sim) obtained using this method were similar to, although about 20−30% larger than, those expected from the ratio ([ClOO] + [Cl])/[ClOO]. The fact that the correction factors are slightly larger than expected from the ratio ([ClOO] + [Cl])/[ClOO] is explained by the fact that the system never quite reaches equilibrium with [Cl] always exceeding, and [ClOO] always below, that expected at equilibrium. It is an unfortunate, but unavoidable, fact that for experiments conducted under conditions relevant to the lower stratosphere (approximately 100 Torr, 215 K) the correction factors to account for the equilibrium between Cl and ClOO are substantial (varying from 3.8 for 205 K to 13.7 for data at 243 K).

Table 1 provides a listing of the rate constants k_2 obtained after correction for the two complications noted above. Quoted uncertainties in Table 1 include statistical uncertainties in data plots such as that shown in Figure 3 and systematic uncertainties associated with the corrections applied (based upon the work of Suma et al.[1] we assume 15% uncertainty in k_1/k_{-1}). As seen from Table 1, within the admittedly large uncertainties, there is no discernible effect of temperature on k_2 for the limited range of temperature, 205−243 K. Variation of the total pressure over the range 50−150 Torr of O_2/N_2 diluent at 213 K did not reveal any effect of total pressure on k_2.

3.3. Measurement of NO_2 Yield in the ClOO + NO Reaction. As discussed in the Introduction, NO_2, ClNO, and $ClONO_2$ are thermochemically allowed products of the ClOO + NO reaction. Cavity ring-down spectroscopy was used to quantify the NO_2 yield using its characteristic absorption in the 485−491 nm region; $ClONO_2$ does not absorb at wavelengths above 440 nm,[8] and absorption by ClNO is unstructured and 25 times weaker than that of NO_2.[24]

CRDS product spectra recorded 1.5 ms after the 355 nm irradiation of $Cl_2/O_2/NO/N_2$ mixtures are shown by the thin lines in Figure 4. The spectra in Figure 4a,b were obtained at 213 K with photolysis laser frequencies of 10 and 2 Hz, respectively. The spectrum in Figure 4c was obtained at 223 K with a photolysis laser frequency of 2 Hz. The thick lines in Figure 4 are NO_2 reference spectra (at the same temperatures as the product experiments) scaled to match the product spectra (thin lines). Comparing the thin and thick lines in Figure 4, one sees that NO_2 is formed in the system. Evidence for NO_2 formation was also observed in experiments performed at 233 and 243 K; however, the lower ClOO concentrations and corresponding weak product absorption precluded a quantitative analysis. Control experiments were performed to check for possible formation of NO_2 from irradiation of mixtures of NO and O_2. The 355 nm irradiation of a mixture of 4.3×10^{18} molecule cm^{-3} of O_2 and 1.6×10^{15} molecule cm^{-3} of NO at 213 K did not give any discernible absorption at 485−491 nm.

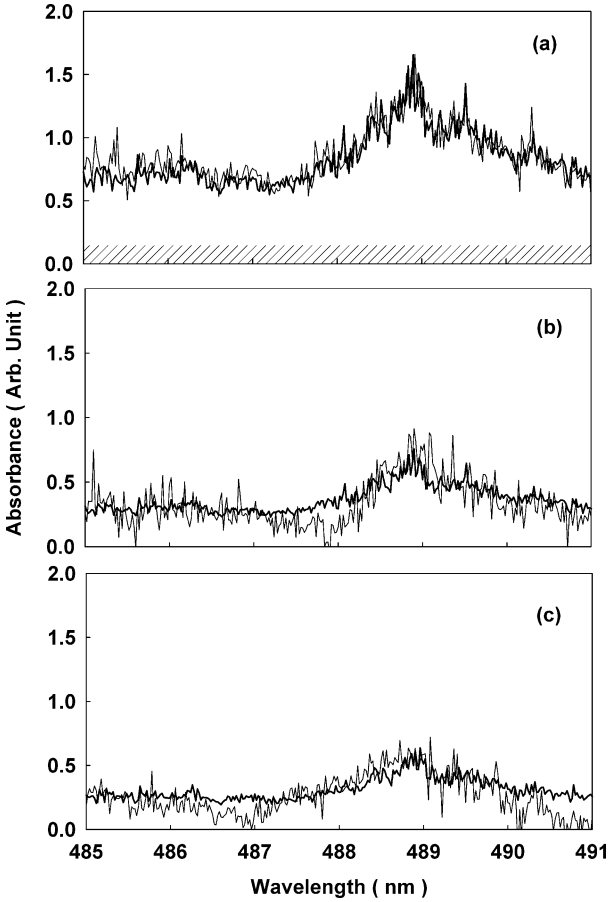

Figure 4. Product spectra (thin lines) recorded 1.5 ms after the 355 nm irradiation of $Cl_2/O_2/NO/N_2$ mixtures in experiments conducted at either 213 K (a), (b) or 223 K (c). The thick lines are NO_2 reference spectra scaled to match the product absorption. The hashed area in panel (a) is attributed to absorption by ClNO. The 355 nm photolysis laser was operated at either 10 Hz (a) or 2 Hz (b), (c).

The product spectrum in Figure 4a is more intense than those in Figure 4b,c because, when a photolysis laser frequency of 10 Hz is used, the gas mixture in the cell is exposed to multiple photolysis laser pulses and the product accumulates in the cell. The spectra shown in Figure 4b,c were obtained with a 2 Hz repetition rate, which provides sufficient time for the products to leave the flow cell between photolysis laser pulses.

To measure the yield of NO_2 in the system, the reference spectra were scaled to provide the best fit to the product spectra, as shown in Figure 4. Interestingly, it was found that the best fits were obtained if we assumed the product spectra to be composed of two spectral components: the structured spectrum of NO_2 and an unstructured absorption. The hashed area in Figure 4a shows the unstructured absorption component, giving the best fit for this experiment. It seems reasonable to assume that the unstructured absorption component reflects the forma-

TABLE 2: Reaction Mechanism Used in ClOO + NO Reaction

reaction	rate constant (cm^6 $molecule^{-2}$ s^{-1} or cm^3 $molecule^{-1}$ s^{-1} or s^{-1})	ref
$Cl + O_2 + M \rightarrow ClOO + M$	$2.7 \times 10^{-33}(T/298)^{-1.5}$	8
$ClOO + M \rightarrow Cl + O_2 + M$	$2.8 \times 10^{-10} \exp(-1819/T)$	25
$ClOO + Cl \rightarrow 2\,ClO$	1.2×10^{-11}	8
$ClOO + Cl \rightarrow Cl_2 + O_2$	2.3×10^{-10}	8
$ClOO + NO \rightarrow ClO + NO_2$	$Y_{NO_2} \times 4.5 \times 10^{-11}$	*a*
$ClOO + NO \rightarrow ClNO + O_2$	$(1 - Y_{NO_2}) \times 4.5 \times 10^{-11}$	*a*
$Cl + ClNO \rightarrow Cl_2 + NO$	$5.8 \times 10^{-11} \exp(100/T)$	8
$ClO + NO \rightarrow Cl + NO_2$	$6.4 \times 10^{-12} \exp(290/T)$	8
$Cl + NO + M \rightarrow ClNO + M$	$9.0 \times 10^{-32}(T/300)^{-1.6}$	8
$2ClOO \rightarrow Cl_2 + 2O_2$	1.6×10^{-11}	10
$ClOO \rightarrow$ diffusion	4.0×10^3	*b*

[a] Y_{NO_2} is the branching ratio for the NO_2 formation in ClOO + NO reaction. [b] Loss of ClOO via diffusion from the viewing zone was obtained from the *y*-axis intercept in the second-order plots (e.g., Figure 3).

tion of ClNO as a product in the system. It should be noted that the absorption cross section of ClNO is much smaller than that of NO_2 by a factor of about 25[24] and the relatively small absorption shown in Figure 4a does not imply that ClNO is a minor product.

We also note that in the calibration of the NO_2 reference spectra shown by the thick lines in Figure 4, allowance was made for NO_2 dimerization using the reported equilibrium constant. However, when considering the product spectra (thin lines in Figure 4), we can neglect NO_2 dimerization because conversion into N_2O_4 is calculated to remove <1% of the product NO_2 on the experimental time scale.

The equilibrium between ClOO and Cl and the consequent presence of Cl atoms is a potential complication, which needs to be considered in the determination of the branching ratio for NO_2 formation, $Y_{NO_2} = k_{2a}/k_2$, from the observed NO_2 formation. There are two source of ClO radicals in the system: reaction of ClOO with Cl and reaction of ClOO with NO via channel (2a). ClO radicals react rapidly with NO giving NO_2 and regenerating Cl atoms.

$$ClOO + NO \rightarrow ClO + NO_2 \qquad (2a)$$

$$ClO + NO \rightarrow Cl + NO_2 \qquad (7)$$

$$Cl + ClOO \rightarrow 2ClO \qquad (8)$$

To investigate the potential complications caused by such secondary reactions in the system, the experimentally observed rise profiles for NO_2 were simulated using the mechanism given in Table 2. Temporal profiles of NO_2 were measured at 489 nm in experiments at 213 K using gas mixtures with $[O_2] = 4.0 \times 10^{18}$, $[N_2] = 4.7 \times 10^{17}$, $[Cl_2] = 1.9 \times 10^{16}$, and $[NO] = 1.6 \times 10^{15}$ molecule cm^{-3}. The contribution of ClNO absorption to these data was included. The chemistry occurring in the system was simulated using the IBM Chemical Kinetics Simulator Software. The initial Cl atom concentration was calculated from $[Cl_2]$ and the photolysis laser power as described in section 2.1. The only parameter varied in the fitting procedure was the branching ratio, $Y_{NO_2} = k_{2a}/k_2$, which was varied to fit the limiting NO_2 plateau at times >0.3 ms (see Figure 5). It is gratifying that the fit shown as the curve through the data points in Figure 5 reproduces both the limiting NO_2 concentration and the kinetic behavior; the observed rate of NO_2 formation is consistent with the value for k_2 derived from observing the ClOO loss. The thin curve close to the *x*-axis in Figure 5 is the predicted NO_2 formation with $Y_{NO_2} = 0$ and represents NO_2 generated from reaction 7 followed by reaction 8. Fortunately, reaction 7 makes only a minor contribution to NO_2 formation. The thick curve in Figure 5 shows the simulated rise of NO_2 using best-fit value of Y_{NO_2} at 213 K of 0.18 ± 0.01. In a similar fashion, a value of $Y_{NO_2} = 0.15 \pm 0.01$ at 223 K was obtained from data with the delay time fixed at 1.5 ms. The uncertainties associated with Y_{NO_2} quoted above reflect statistical uncertainty in the measurement of NO_2. If we account for uncertainties in the initial Cl atom concentration caused by fluctuations of laser power, pressure, temperature, and gas flow rate, we arrive at values of $Y_{NO_2} = 0.18 \pm 0.02$ at 213 K and $Y_{NO_2} = 0.15 \pm 0.02$ at 223 K.

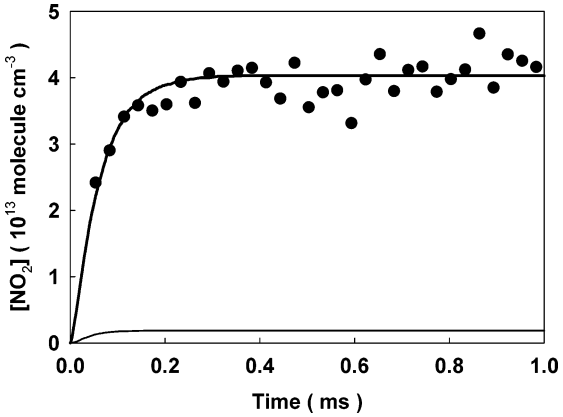

Figure 5. Temporal profile of NO_2 observed in an experiment at 213 K using the following reagent concentrations (molecule cm^{-3}): O_2, 4.0×10^{18}; N_2, 4.7×10^{17}; Cl_2, 1.9×10^{16}; NO, 1.6×10^{15}. The solid circles are experimental results. The thick and thin curves are results of simulations using $Y_{NO_2} = 0.18$ and 0.00, respectively.

4. Discussion

The present work is the first application of CRDS to study ClOO radical reaction kinetics and the first direct study of the ClOO + NO reaction. The reaction proceeds with a rate constant $k(ClOO+NO) = (4.5 \pm 0.9) \times 10^{-11}$ cm^3 $molecule^{-1}$ s^{-1} at 213 K. There is no discernible effect of temperature on the rate of reaction over the range studied (205−243 K); see Table 1. NO_2 was observed as a reaction product and branching ratios of $k_{2a}/k_2 = 0.18 \pm 0.02$ at 213 K and $k_{2a}/k_2 = 0.15 \pm 0.02$ at 223 K were determined. Evidence for the formation of ClNO product was observed in the form of a small featureless residual absorption at 485−491 nm. The magnitude of the residual absorption is consistent with ClNO being a major product, perhaps accounting for the balance of reaction, i.e., $k_{2b}/k_2 \approx 0.8$. However, in light of uncertainties associated with quantification of the residual absorption, this should be regarded as a tentative conclusion.

It is of interest to compare our results for reaction 2 with the database for reactions of other peroxy radicals with NO. It is well established that reaction of HO_2 and alkyl peroxy radicals (e.g., CH_3O_2, $C_2H_5O_2$) with NO proceed with a rate constant of approximately 1×10^{-11} cm^3 $molecule^{-1}$ s^{-1} at the temperatures employed in the present work.[8] Acyl peroxy radicals (e.g., $CH_3C(O)O_2$) react more rapidly with NO with rate constants approaching 3×10^{-11} cm^3 $molecule^{-1}$ s^{-1} at 220 K. ClOO radicals are more reactive toward NO than any other peroxy radical yet studied. The absence of any pronounced dependence of k_2 on temperature is consistent with the behavior of HO_2 and organic peroxy radicals whose reaction kinetics display weak negative temperature dependencies consistent with the reaction proceeding via formation of an intermediate adduct.

The dominant products of the reaction of HO_2 and organic peroxy radicals with NO are the corresponding oxy radical and NO_2 (e.g., $CH_3O_2 + NO \rightarrow CH_3O + NO_2$). There is an analogous reaction channel in the ClOO + NO reaction, but it is a minor, $k_{2a}/k_2 = 0.18 \pm 0.02$ at 213 K, not dominant, channel. The dominant channel in the ClOO + NO reaction appears to give ClNO. The different behavior probably reflects either the weak Cl−O bond in ClOO and ease with which ClNO could be eliminated from the ClOONO adduct or the existence of a direct abstraction channel in the ClOO + NO reaction in which the incoming NO can abstract the Cl atom. Ab initio studies are needed to distinguish between these possibilities.

It is of interest to compare reaction 2 with the analogous reaction of FO_2 radicals. The FO_2 + NO reaction proceeds slowly, $k = 3 \times 10^{-13}$ cm^3 molecule^{-1} s^{-1} at 220 K, with kinetics that display a positive temperature dependence ($E_a/R = 690$), giving FNO and O_2 as products.[8] There are two significant differences between FO_2 and ClOO that can explain their different reactivities toward NO. First, the F−O bond strength in FO_2 is approximately 54 kJ mol^{-1} and is much stronger than the Cl−O bond in ClOO, 19.5 kJ mol^{-1}. Second, the reaction channel to give XO + NO_2 is endothermic for FO_2 but exothermic for ClOO. Ab initio studies of the reactions of FO_2 and ClOO with NO would be useful in providing a more fundamental understanding of these reactions.

Finally, it should be noted that given the reactive nature of Cl atoms toward the large amounts of ozone in the stratosphere ($k(Cl+O_3) = 1 \times 10^{-11}$ cm^3 molecule^{-1} s^{-1} at 220 K, $[O_3] = 10^{12}-10^{13}$ molecule cm^{-3} at 10−20 km) and the relatively small fraction of Cl atoms that is tied up in the form of ClOO radicals (see Introduction), reaction of ClOO with NO (or any other species) does not play a significant role in atmospheric chemistry.

Acknowledgment. We are grateful to Prof. S. Aloisio of California State University for helpful discussion. This work is supported partly by grants from the 21st Century COE project of Kyoto University, and the Yazaki Foundation. S.E. thanks the JSPS Research Fellowship for Young Scientists.

References and Notes

(1) Suma, K.; Sumiyoshi, Y.; Endo, Y.; Enami, S.; Aloisio, S.; Hashimoto, S.; Kawasaki, M.; Nishida, S.; Matsumi, Y. *J. Phys. Chem. A* **2004**, *108*, 8096.

(2) Suma, K.; Sumiyoshi, Y.; Endo, Y. *J. Chem. Phys.* **2004**, *121*, 8351.

(3) Gane, M. P.; Williams, N. A.; Sodeau, J. R. *J. Chem. Faraday. Trans.* **1997**, *93*, 2747.

(4) Zhu, R. S.; Lin, M. C. *J. Chem. Phys.* **2003**, *119*, 2075.

(5) Li, Q.; Lu, S.; Xu, W.; Xie, Y.; Schaefer, H. S., III. *J. Phys. Chem. A* **2002**, *106*, 12324.

(6) Thomsen, C. L.; Philpott, M. P.; Hayes, S. C. *J. Chem. Phys.* **2000**, *112*, 505.

(7) Finlayson-Pitts, B. J.; Pitts Jr., J. N. *Chemistry of the Upper and Lower Atmosphere: Theory, Experiments and Application*s; Academic Press: San Diego, CA, 2000.

(8) Sander, S. P.; Friedl, R. R.; Ravishankara, A. R.; Golden, D. M.; Kolb, C. E.; Kurylo, M. J.; Huie, R. E.; Orkin, V. L.; Molina, M. J.; Moortgat, G. K.; Finlayson-Pitts, B. J. Chemical Kinetics and Photochemical Data for Use in Stratospheric Modeling; Evaluation 14, Jet Propulsion Laboratory: Pasadena, CA, 2003.

(9) U.S. Standard Atmosphere, 1976, NOAA, NASA, USAF, Washington, DC, 1976.

(10) Baer, S.; Hippler, H.; Rahn, R.; Siefke, M.; Seitzinger, N.; Troe, J. *J. Chem. Phys.* **1991**, *95*, 6463.

(11) Mauldin, R. L.; Burkholder, J. B.; Ravishankara. A. R. *J. Phys. Chem.* **1992**, *96*, 2582.

(12) Nicovich, J. M.; Kreutter, K. D.; Shackelford, C. J.; Wine, P. J. *Chem. Phys. Lett.* **1991**, *179*, 367.

(13) O'Keefe, A.; Deacon, D. A. G. *Rev. Sci. Instrum.* **1988**, *59*, 2544.

(14) Wheeler, M. D.; Newton, S. M.; Orr−Ewing, A. J.; Ashfold, M. N. R. J. *Chem. Soc., Faraday Trans.* **1998**, *94*, 337.

(15) Berden, G.; Peeters, R.; Meijer, G. *Int. Rev. Phys. Chem.* **2000**, *19*, 565.

(16) Yu, T.; Lin M. C. *Int. J. Chem. Kinet.* **1993**, *25*, 875.

(17) Yu, T.; Lin M. C. *J. Phys. Chem.* **1995**, *99*, 8599.

(18) Ninomiya, Y.; Goto, M.; Hashimoto, S.; Kawasaki, M.; Wallington, T. J. *Int. J. Chem. Kinet.* **2001**, *33*, 130.

(19) Ninomiya, Y.; Goto, M.; Hashimoto, S.; Kagawa, Y.; Yoshizawa, K.; Kawasaki, M.; Wallington, T. J.; Hurley, M. D. *J. Phys. Chem. A* **2000**, *104*, 7556.

(20) Nakano, Y.; Goto, M.; Hashimoto, S.; Kawasaki, M.; Wallington, T. J. *J. Phys. Chem. A* **2001**, *105*, 11045.

(21) Nakano, Y.; Enami, S.; Nakamichi, S.; Aloisio, S.; Hashimoto, S.; Kawasaki, M., *J. Phys. Chem. A.* **2003**, *107*, 6381.

(22) Atkinson, D. B.; Hudgens, J. W. *J. Phys. Chem. A* **1997**, *101*, 3901.

(23) Brown, S. S.; Ravishankara, A. R.; Stark, H. J. *J. Phys. Chem. A* **2000**, *104*, 7044.

(24) Roehl, C. M.; Orlando, J. J.; Calvert, J. G. *J. Photochem. Photobiol. A: Chem.* **1992**, *69*, l.

(25) Atkinson, R.; Baulch, D. L.; Cox, R. A.; Hampson, R. F., Jr.; Kerr, J. A.; Rossi, M. J.; Troe, J. *J. Chem. Phys. Ref. Data* **1997**, *26*, 521.